nature chemistry

SUPPLEMENTARY INFORMATION

DOI: 10.1038/NCHEM686

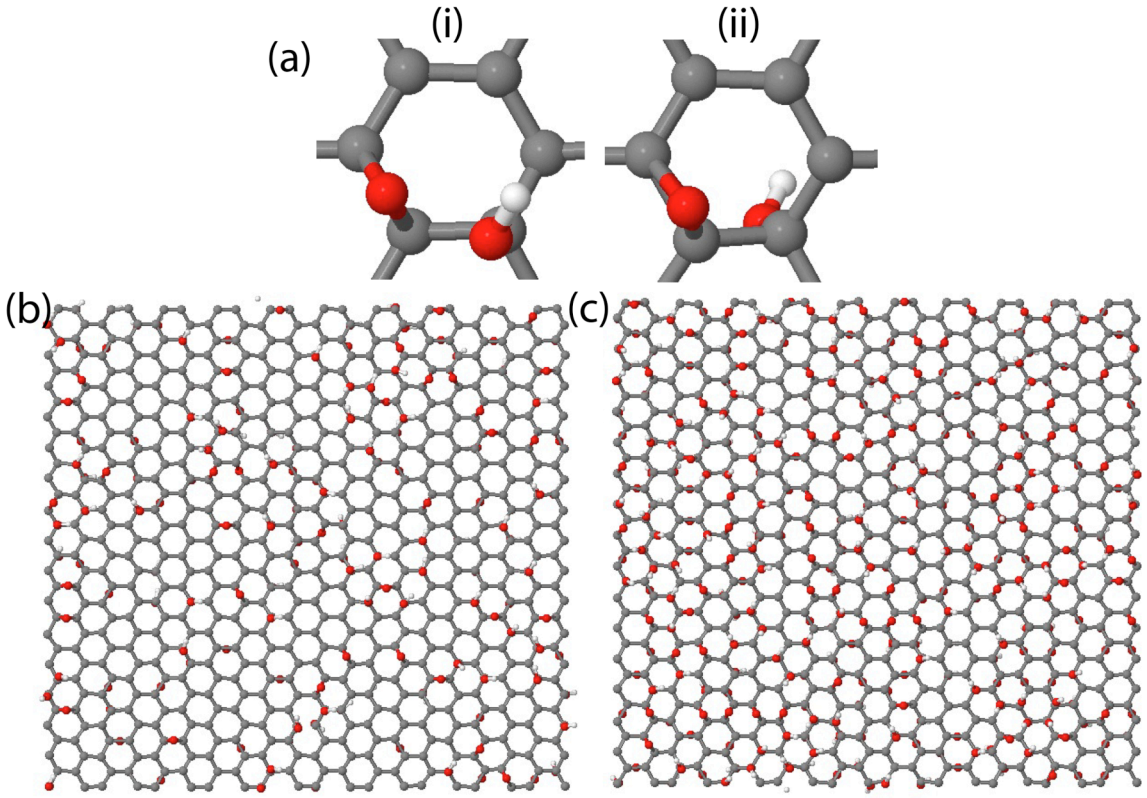

Figure S1: (a) Initial configuration of hydroxyl and epoxy groups used in the MD calculations based on the observations of Cai et al. [Ref [27] in the MS] who found that hydroxyl and epoxy groups are bonded to neighboring carbon atoms. The hydroxyl group is on the same side of the basal plane in (i) while it is on the opposite side in (ii). Similarly, the epoxy group can be on either side of the basal plane (not shown). Initial configuration of simulated GO structures for (b) 20% (c) 33% oxygen in the form of hydroxyls and epoxys in the ratio of 3:2 at 300 K. The final morphologies after annealing are given in Fig. 1 of the MS. Carbon, oxygen and hydrogen atoms are color-coded as gray, red and white, respectively.

The MD simulations were performed on a variety of hydroxyl to epoxy ratios and concentrations. To complete the series considered for 3:2 (hydroxyl:epoxy) ratio at

DOI: 10.1038/NCHEM686

different oxygen concentrations, the initial distribution of oxygen atoms and the annealed structures of graphene oxide (GO) containing 25% oxygen are shown in Fig. S2.

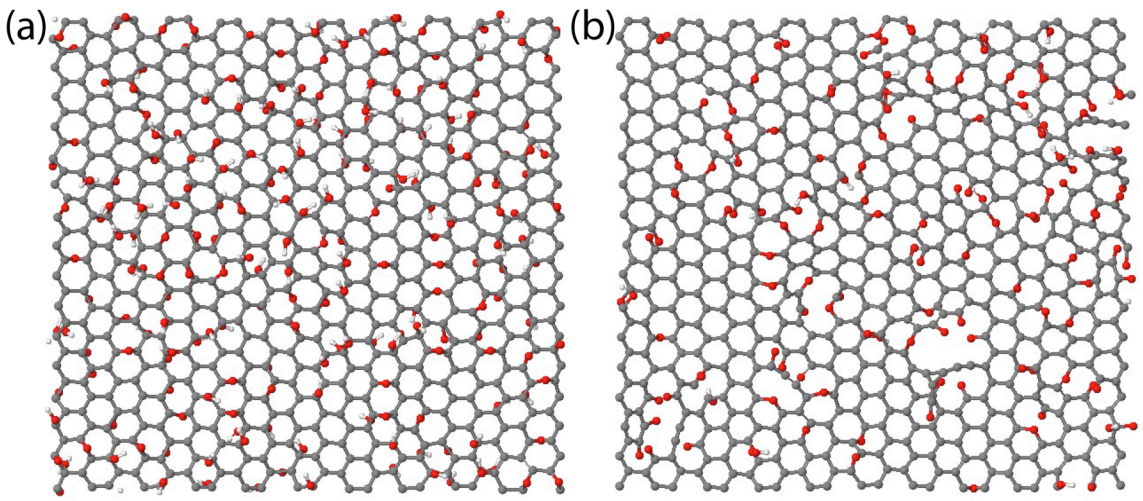

Figure S2: Structure of GO sheet with hydroxyl to epoxy ratio of 3:2 with 25% oxygen concentration (a) before and (b) after annealing at 1500K.

The side views of the initial and post annealed GO sheets were investigated to study the roughness induced by the evolution of oxygen functional groups. The initial configurations of GO sheets used in our simulations are free of the ripples observed in pure graphene sheets. However, ripples (or roughness) can clearly be seen after reduction, as indicated in Fig. S3b and d. The longest wavelength of the ripples observed was half the size of the simulation cell. For a given amplitude, A, the curvature associated with a ripple of wavelength L is AL^{-2} and since the bending energy scales with square of curvature, longer wavelength ripples will have lower energies associated with them. Since longer wavelength ripples include relatively smaller deformation, they should not significantly influence the chemical reactions we have observed.

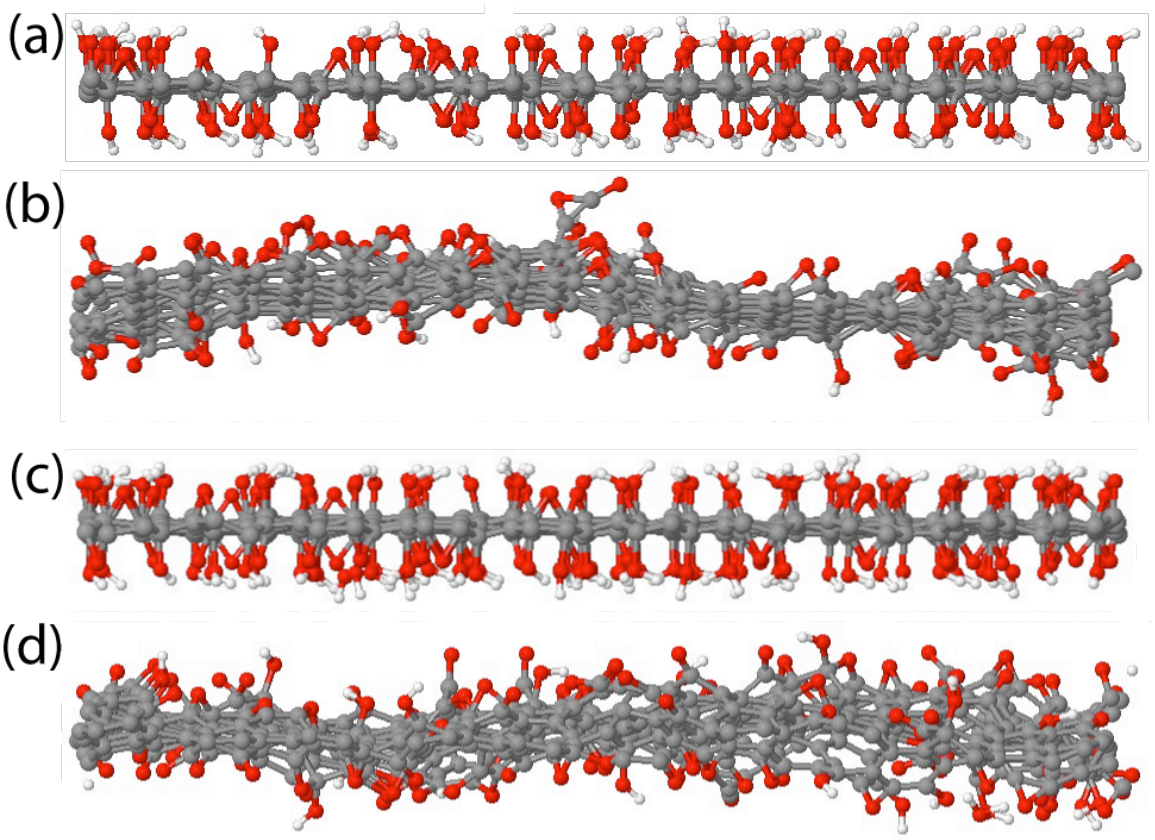

Figure S3: Side views of GO sheets with hydroxyl to epoxy ratio of 3:2 at oxygen concentrations of 20% (a,b) and 25% (c,d). (a) and (c) correspond to the configurations before reduction, while (b) and (d) are the configurations after reduction.

DOI: 10.1038/NCHEM686

The mechanisms for creation of stable residual oxygen functional groups were investigated. The process paths for the creation of residual oxygen in basal plane in the presence of hydroxyls and epoxies (Fig. S4) and when only epoxies are present (Fig. S5) are shown below. The key steps in these reactions involve 1) formation of the carbonyl groups, 2) transfer or hopping of hydrogen atoms between different hydroxyl groups and carbonyl or epoxy groups and 3) formation of new bonds between oxygen atoms that are part of carbonyl groups and under-coordinated carbon atoms in the basal plane.

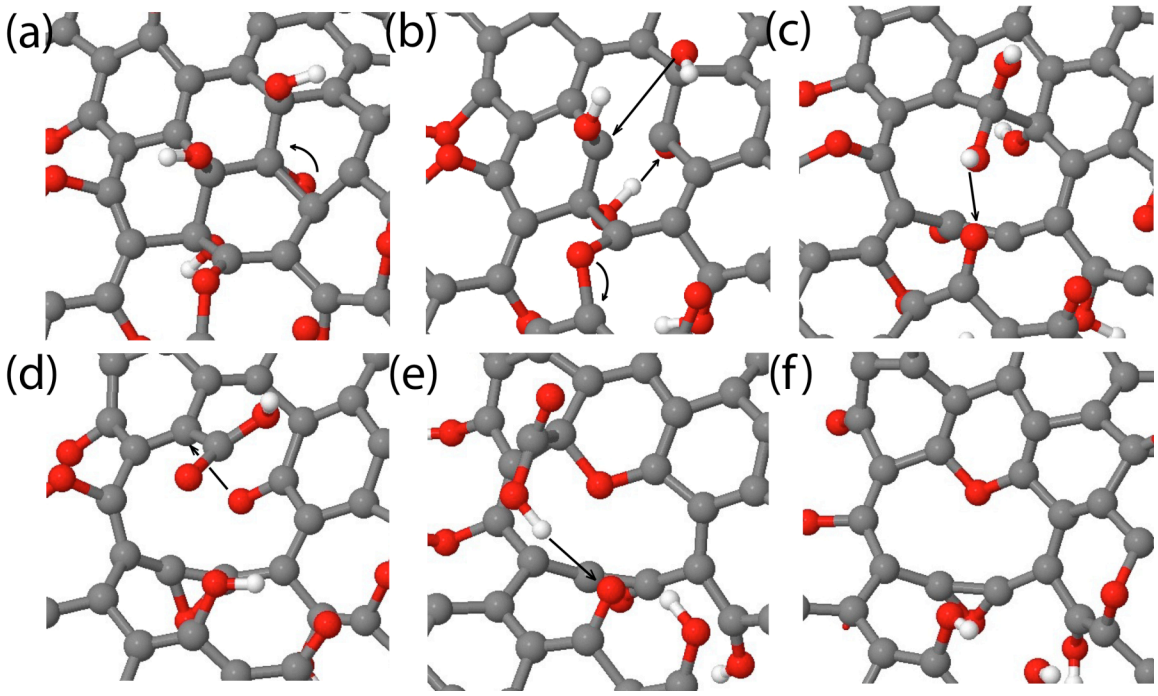

Figure S4: (a) Initial configuration with hydroxyl and epoxies that leads to the incorporation of an oxygen atoms in the basal plane (f). The ephemeral intermediate configurations seen in the MD simulations are shown in panels b – e. The sequence of events resulting in the incorporation of the oxygen molecule in the basal plane are: 1) Formation of a carbonyl –phenol hole (b), 2) Transfer of hydrogen via hydrogen bonding (b-c), 3) Formation of carboxyl group (d) Hydrogen migration and release of CO_2 (e-f).

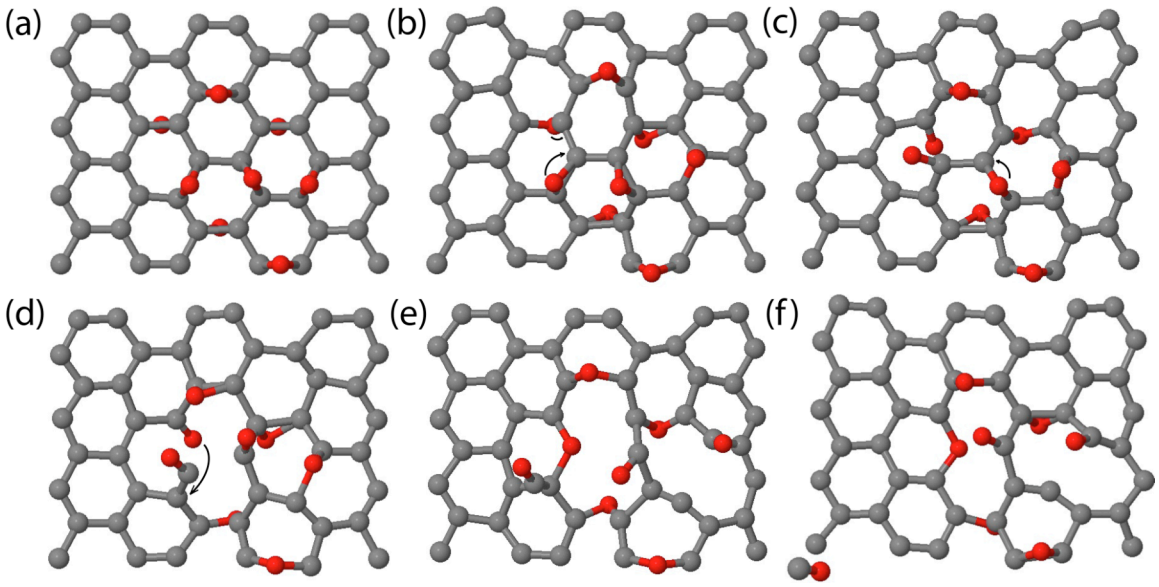

Figure S5: (a) Initial configuration with epoxies only that leads to the incorporation of oxygen atom in the basal plane (f). A CO molecule is produced as a byproduct of this reaction (refer panel (e)). The ephemeral intermediate configurations that facilitate the formation this molecule and the pyran configuration are indicated in panels b – e. The sequence of events shown in the figure are: 1) breaking the C-O bonds shown arrows in (b) leading to the creation of a hole decorated by carbonyl pair shown in (c). 2) formation of an atop C-atom leading to C-C bond breaking and creation of an out-of-plane C=O configuration as shown in (d). 3) connection of the oxygen which is part of carbonyl to the under-coordinated carbon atom in (e) resulting in the formation of a CO molecule as shown in (f).

We briefly discuss the issue of cell size separately for a) the first principles calculations that were used to compute the formation energies and energy barriers for ketone and phenol groups (Fig. 3 of main text) and b) molecular dynamics simulations of thermal annealing.

In our first principles calculations, we tested the effect of system size two ways. First the size of the supercell with the epoxy, hydroxyl and carbonyl groups in Fig. 3 of the main text was progressively increased from 1.28 nm x 0.98 nm to 2.13 nm x 1.48 nm to ensure that the formation energies are not influenced by finite size effects. Next, for a given supercell, we carried out cell optimization to obtain the correct size. With this procedure,

DOI: 10.1038/NCHEM686

we have ensured that the strain in the C-C bonds at the boundary of the super cell is indeed negligible for the results reported in Fig. 3 of the MS.

To study the effect of cell size on the morphology of GO sheets and the distribution of functional groups, we have also first equilibrated the simulation using an NPT ensemble with the Nosé-Hoover thermostat and barostat for temperature and pressure control, respectively, at a time step of 0.25 fs. The supercell was first gradually heated from 10 K to 1000 K over a time span of 625 fs, then annealed at 1000 K for 625 fs, and subsequently quenched to 300 K over a time span of 625 fs. Finally, the supercell was further annealed at 300K and zero pressure for the duration of 4.25 ps to ensure complete equilibration of the structure. After this equilibration phase, we switched to an NVT ensemble at the appropriate reduction temperature. We have found no significant difference in the results with this procedure for cell relaxation compared to the simpler approach presented in the article. This can be understood by considering the energetic driving force for the formation of carbonyls and phenol groups as revealed by our first principles calculations (Fig. 3) –- the strain in the C-C caused by the epoxides is relaxed by the formation of carbonyls and ethers. Once these groups are formed, other C-C bonds in their vicinity return to their normal lengths.

The simulations show that after 200ps the rate of formation of defects and other byproducts decreases considerably. This is compatible with the experimental observation in Ref. [6] in the MS that indicates that the oxygen removal rate above 723K decreases substantially. The reason is the formation of carbonyls and the other stable configurations such as furans and pyrans, which cannot be removed by further thermal annealing. Thus, annealing for a longer time than 200ps results in no major difference in morphology and structure. The structure shown in Fig.1b is actually obtained after annealing at 1500K for 250ps with an initial oxygen concentration of 33%. Finally, in order to confirm the stability of the different configurations, the GO sheet was cooled to 300 K in 1.25ps and annealed at this temperature for 1.25 ps

The influence of the heating velocity on the simulation results was also investigated. Upon heating the sheets with the initial distribution of functional groups from 300 K to typical reducing temperatures (> 1000 K), the first reactions that we observe are the

formation of water molecules (e.g. Fig. 3a in the main MS) and desorption of hydroxyls. If the heating is done very slowly, then several of these byproducts will be released before reaching 1000 K. The heating velocity was carefully chosen so that significant amounts byproducts are not released, yet not subjecting the system to a large thermal shock (i.e. allowing the morphology to evolve as gradually as possible).

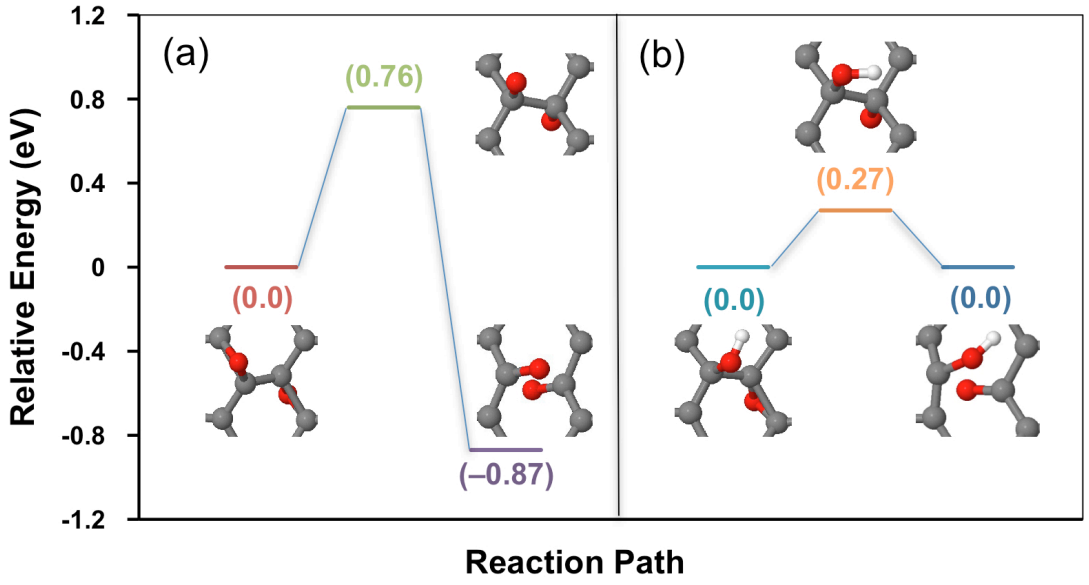

Figure S6: Energy barriers and transition states for the formation of (a) a carbonyl pair from a pair of epoxies and (b) a phenol-carbonyl pair from hydroxyl and epoxy groups. The transition states in both cases are characterized by "atop" oxygen atoms on the basal plane.

Comparison of our results with other works

Our initial configurations consist of randomly distributed hydroxyl and epoxy groups, which should allow for defect formation as well as for the production of CO, CO_2 and H_2O as seen in experiments. In this regard, our simulations are very much similar to what is done for hydrogenated graphene in Ref. [S1]. The work in Ref [S2] assumes an idealized structure (H-atoms attached to all C-atoms) whereas in Ref [S1] H-domains grow in a random manner leading to "frustration". Our work is consistent with that of Ref. [S1].

Our work is consistent with that of Ref. [S3] In both our work and in Ref. [S3], large "holes"

DOI: 10.1038/NCHEM686

are formed in GO sheets, which eventually leads to fracture of the sheets. However in Ref. [S3] this is attributed to the alignment of epoxies a perfect row, but in our simulations this sort of perfect alignment is not necessary. However, as pointed out by Ajayan and Yakobson[S3], it is not clear how isolated epoxy groups fall into ranks to take part in a well orchestrated serial bond-breaking and rebonding process that leads to the formation of the epoxy rows. The randomly-bound epoxy groups can only find such stable alignments as a result of rapid vacillation between different sites, but this is not easy to reconcile with the high energy barriers associated with such a mechanism, which can be of the order of a few eV. In distinct contrast to holes formed at the epoxy chains, the holes formed in our simulations arise solely from the random arrangement of epoxy and hydroxyl groups.

XPS Results

The real GO samples used in this study are identical to the ones used in our work in Ref. 5, 6 in the MS. Detailed structural and chemical analyses and opto-electronics properties of the GO thin films as a function of the degree of reduction are reported in that work. We therefore refer to that work for further details.

C 1s peaks collected after annealing at 573 and 723 K corresponding to the O 1s reported in the MS are shown in Fig. S7. The C 1s component has been deconvolved in five components [S4-5:] C=C/C-C in aromatic rings (284.6 eV); C-O (285.8 eV); C=O (286.9 eV); C(=O)-(OH) (288.7 eV); and π-π* satellite peak (290.6 eV). The carbon sp^2 component area is 70% of the total C1s peak area. Rest of the components have an area of: 16.3% for C-O, 13.3% for C=O and 0.4% for C(=O)-(OH). The Oxygen bound to a valence carbon, can be present in the form of epoxide or hydroxyl. In the case of epoxides, each oxygen atom bears two carbon atoms. Therefore considering the case wherein hydroxyls and epoxides are present in an equivalent amount, oxygen present in the form carbonyl component represents 47% of the total oxygen. On the other hand, if we consider an excess of epoxides (25% more than hydroxyls), the percentage of carbonyls can rise up to 49%. Therefore the total concentration of carbonyl and carboxyl groups added up represents ~ 50 % of the total oxygen, which is in agreement with the concentration found from O 1s peak.

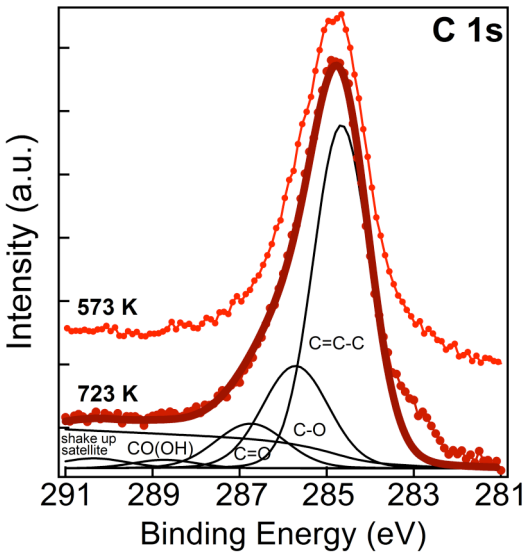

Figure S7: C 1s XPS spectra (hν=1253.6 eV) collected on single layered GO deposited on Au(10nm)/SiO_2(300nm)/Si and annealed in UHV at the indicated temperatures for 15 min. The spectra were fit by Doniach-Sunjic function after subtracting a Shirley background (as in the case of O 1s spectrum) and the different components related to various chemical shifts of carbon bonds are indicated.

References

1 Flores, M. Z. S., Autreto, P. A. S., Legoas, S. B. & Galvao, D. S. Graphene to graphane: a theoretical study. *Nanotechnology* **46**, 465704 (2009).

2 Sofo, J. O., Chaudhari, A. S. & Barber, G. D. Graphane: A two-dimensional hydrocarbon. *Phys. Rev. B* **75**, 153401 (2007).

3 Li, J.-L. *et al.* Oxygen-driven unzipping of graphitic materials. *Phys. Rev. Lett.* **96**, 176101 (2006).

4 Yumitori, S. Correlation of C1s chemical state intensities with the O1s intensity in the XPS analysis of anodically oxidized glass-like carbon samples *J. Mater.Sci.* **35**, 139 (2000).

5 Briggs, D. & Seah, M. P. *Practical surface analysis*. (John Wiley & Sons Ltd, 1983).